# Advances in measuring linear viscoelastic properties using novel deformation geometries and Fourier transform techniques

**Howard See**

*School of Aerospace, Mechanical & Mechatronic Engineering,*
*The University of Sydney, NSW 2006, Australia*

## Abstract

The development of new techniques for the dynamic measurement of linear viscoelastic properties is an active area of rheometry, and this paper surveys some novel deformation geometries which have been recently reported e.g. oscillating probe-type devices which are imbedded in or placed on the surface of the sample. Small amplitude band-limited pseudorandom noise is used for the displacement signal, with Fourier analysis of the complex waveform of the resistance force yielding the frequency dependent viscoelastic material functions (e.g. storage and loss moduli $G'$, $G''$). Theoretical calculations of the fundamental equations relating force to displacement and instrument geometry, were carried out with the aid of the correspondence principle of linear viscoelasticity. The rapidity of the tests and flexibility in terms of sample preparation and stiffness mean that this basic technique should find many applications in rheometry. Three examples of oscillatory tests are presented in detail : squeeze flow, imbedded needle and concentric sliding cylinder geometries.

*Keywords* : linear viscoelasticity, correspondence principle, pseudorandom noise strain, squeeze flow, needle

## 1. Introduction

Dynamic measurements of linear viscoelastic properties are a common way to characterise the rheological nature of a material. In general, the tests involve applying a harmonic displacement (or a harmonic force) to a bounding surface of the sample, and measuring the material's response to this excitation via the resistance force signal (displacement signal). The force and displacement amplitudes are assumed to be small so the sample responds in the linear viscoelastic regime, enabling determination of material functions such as the storage modulus $G'(\omega)$ and loss modulus $G''(\omega)$, which are functions of the oscillation frequency $\omega$. A great variety of rheometer designs can be used for measuring linear viscoelastic properties, and in this paper we will survey some recently developed novel deformation geometries, e.g. probe-type devices which are imbedded in or placed on the surface of samples. These novel geometries have proved to be very useful in particular application situations, such as small sample volumes, sheet-like samples, or solid-like samples which are difficult to prepare for conventional tests. Another devel-

opment which will be reviewed in this paper is the use of pseudorandom noise signals for the displacement, taking advantage of the linear nature of the sample's response to impose a range of harmonic frequencies simultaneously, with Fourier analysis of the resulting response signals identifying the individual frequency components.

Extensive reviews of the many techniques developed for the measurement of linear viscoelastic properties appear in the books by Walters (1975), Hutton *et al.* (1975), Ferry (1980), Whorlow (1992), Macosko (1994), Collyer and Clegg (1998). These techniques range from conventional rotational rheometers (parallel plate, cone-plate, concentric cylinders) where small amplitude oscillations in angular displacements and torques are used as the basis of the measurement, up to highly specialised devices such as the Metravib instrument where electromagnets are used to induce torsional oscillations in rod-like samples (see e.g. Whorlow, 1992). An interesting class of rheometers for measuring linear viscoelastic properties was developed in the 1960's and 1970's, which involved *steady* rotation of appropriate boundaries in the test geometries, resulting in harmonic deformation of each fluid element in the sample (see the review in Walters, 1975). Examples include the rotating cantilever method and the orthogonal rheometer, in which the sample was sandwiched between two rotating

parallel discs with eccentric rotation axes. Two instruments closely related to the techniques to be discussed in this paper are the vibrating probe curemeter (Pethrick, 1993; 1998) and the paddle rheometer, which uses an oscillating immersed paddle (Banfill *et al.*, 1991; Affrossman *et al.*, 1990; Radhakrishnan and Pethrick, 1994; Pethrick, 1993; 1998). These rheometers are able to characterise the viscoelastic behaviour of a wide variety of materials, but they do not appear to have a theoretical framework for the force-displacement equation and so require careful calibration with a known standard fluid.

The methods for measuring linear viscoelastic properties described above typically impose a sinusoidal excitation at a fixed frequency, and more complex signals are usually not used, although in principle there is no reason why they could not. Indeed, in the techniques to be described in this paper, a band-limited pseudorandom noise signal will be used as the input strain history. It should be noted that some recent commercial rheometers include a "multiwave" oscillatory option whereby the strain signal consists of several superposed sinusoids of different frequencies. Some basic aspects of multiwave testing are discussed in Holly *et al.* (1988), Nelson and Dealy (1993; 1998). The band-limited pseudorandom noise technique to presented in this paper can be considered an extension of this multiwave method, although, in comparison, the random noise approach can produce many more data points in the frequency domain, for example 1 Hz to 100 Hz at 0.5 Hz intervals. A large number of data points is desirable, for example, if numerical inversion is to be carried out to obtain the relaxation time spectra (e.g. using the regularisation technique of Honerkamp and Weese, 1993). The combination of these complex waveforms and Fourier analysis allows for very rapid but detailed measurements of the linear viscoelastic properties, permitting close monitoring of changes in properties over time, an issue of interest when dealing with curing or setting materials (e.g. Gonsalkorale *et al.*, 1999; Jiang *et al.*, 2001). It should be pointed out that with all these techniques, the oscillation frequencies cannot be too high (usually less than 100 Hz) otherwise inertia effects will influence the results (section 4.1).

From the viewpoint of rheometer construction, although in principle a pseudorandom noise displacement signal can be used in any rheometer geometry, its use in some particular configurations has recently become a practical possibility due to the development of accurate motion control systems, such as the giant magnetostrictive Terfenol driver system described in section 3. Further, software and motion control technology have now advanced to the stage where band-limited pseudorandom noise signals can be efficiently generated, with fast Fourier algorithms capable of analysing the force signals in real time yielding the frequency dependent material functions. Note that even with present

technology, a system based on pseudorandom noise displacements could still be difficult to incorporate in conventional rotational rheometers due to limitations in motor design and control.

In addition to the band-limited pseudorandom noise as the input displacement signal, this paper will describe the use of small probe-type instruments of different geometries (e.g. the needle in sect. 3.2), which are well suited to viscoelastic measurements of solid-like samples. Prescribed displacement tests on solid-like materials are difficult to perform on conventional rotational rheometers, since the large torque signals often overload the transducer. On the other hand, the force signals can be kept to much more manageable levels through the use of small oscillating probes with appropriate geometries. Further, the variety in test geometries gives great flexibility in sample volumes or sample preparation : the oscillatory squeeze flow instrument (sect 3.1) requires small samples, whereas the imbedded needle method (sect 3.2) requires minimal preparation of the sample surface and also can be used on small samples.

In general, for any rheometer geometry, it is desirable to have a theoretical framework and the fundamental equation relating force to the displacement and the instrument geometry. As will become clear from the discussion in this paper (Sect. 2.1), a convenient and powerful way to theoretically derive the required force-displacement relation is based on the correspondence principle of linear viscoelasticity. This principle provides a powerful analytical tool for finding the governing equation for the case of a viscoelastic sample, using results obtained from small strain elasticity or steady Newtonian fluid flow analyses.

In this paper we present an overview of basic concepts and recent developments in the use of novel deformation geometries coupled with pseudorandom noise displacement signals and Fourier analysis, to determine the linear viscoelastic properties of a sample. Although the focus will be on the new developments, we will present an introduction to fundamental features which should prove useful to a new entrant in the field. The paper is organised as follows. In section 2 , we describe the key concepts of the correspondence principle of linear viscoelasticity, and the use of pseudorandom noise displacement signals and Fourier transform techniques to extract the viscoelastic material functions. In section 3 we describe three applications which show the utility of this approach : oscillatory squeeze flow (Sect. 3.1), oscillating imbedded needle (Sect 3.2), and oscillating sliding cylinders (Sect. 3.3). The possibility of other deformation geometries is treated in section 3.4. In section 4 we discuss other important issues, such as inertia effects (Sect. 4.1) and the use of large amplitudes to explore non-linear viscoelasticity (Sect. 4.2). Finally, some concluding remarks are presented in section 5.
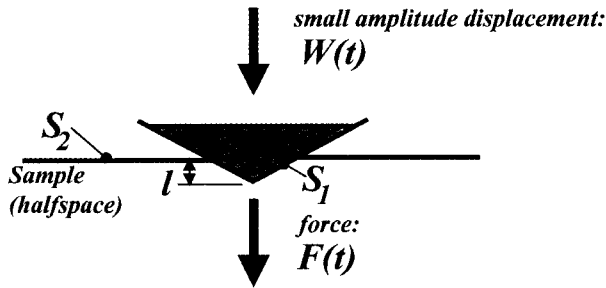
**Fig. 1.** Schematic diagram of the general contact problem. $W(t)$ is the small displacement normal to the surface of the half-space, and $F(t)$ is the resulting resistance force due to the deformed matrix (assuming no slip at the probe-matrix interface).

## 2. Key concepts

### 2.1. Correspondence principle of linear viscoelasticity

To begin we consider the general situation as shown in Figure 1, where a probe is imbedded in a homogeneous elastic matrix. Assume that the probe undergoes a small displacement $W$ from this position, where $W \ll l$, $l$ being a characteristic lengthscale of the imbedded probe geometry. Typically the boundary conditions are no slipping at the probe-matrix interface (perfect adhesion), and zero traction at the free surface. This type of problem is often called a "boundary value contact problem", and for example the resistance force $F$ acting on the probe due to the deformed matrix can be calculated. There are books which have extensive descriptions of these kinds of calculations for elastic matrices (e.g. Johnson, 1987; Hills et al., 1993). The final equation relating the force F to the material's mechanical properties, which we will represent initially as a function $g_{material}$ ($g_{material}$ could be a function of moduli, compressibility, anisotropy, etc), and the displacement W, takes the following general form:

$$F = kg_{material}W \qquad (2.1)$$

Here $k$ is a constant depending on the probe geometry.

Many rheological measurements are performed under the assumption that the sample is isotropic and incompressible (so Poisson's ratio $v = 0.5$). The material's linear mechanical behaviour can then be uniquely characterised by one material parameter, and we will use the elastic shear modulus $G$. Eq(2.1) can thus be rewritten

$$F = kGW \qquad (2.2)$$

We now turn to a discussion of the correspondence principle of linear viscoelasticity, which will be used to obtain a force-displacement relation for the case of a viscoelastic

matrix. Broadly speaking, this principle states that the results calculated for an elastic matrix can also be used for the problem where the same probe (Figure 1) is imbedded in a viscoelastic sample and undergoes small amplitude oscillation $W(t) = W_0e^{i\omega t}$ about a mean position. The essential concept is the direct mathematical correspondence between the governing equations for the Fourier-transformed linear viscoelastic problem and the original small strain elasticity problem with the same boundary conditions. A detailed treatise on the correspondence principle is Bland (1960) (see also Lee et al., 1960; Hashin, 1970; Schapery, 1974; Walters, 1975; Pipkin, 1986; Christensen, 1979; Haddad, 1995; Tanner, 2000).

To illustrate the reasoning behind the correspondence principle, let us consider the small strain contact problem for the case of an incompressible elastic matrix. Writing $\sigma$ for the stress tensor and $\varepsilon$ for the infinitesimal strain tensor, the governing equations are as follows:

(E1) the equation of motion (ignoring body forces and inertia effects)

$$\nabla \cdot \sigma = 0 \qquad (2.3)$$

(E2) Conservation of mass (incompressibility)

$$tr\varepsilon = 0 \qquad (2.4)$$

(E3) Constitutive equation (assuming a Hookean solid, and ignoring an arbitrary isotropic pressure)

$$\sigma = G\varepsilon \qquad (2.5)$$

(E4) Boundary conditions : prescribed displacement at the probe-matrix interface $S_1$ (non-slip); and traction-free at the exposed upper surface $S_2$ (i.e. $\sigma.n = 0$, where $n$ is the unit normal vector at the surface).

We move on to consider the problem of a linear viscoelastic material under a small amplitude sinusoidal deformation of frequency $\omega$: $\varepsilon(t) = \varepsilon_0e^{i\omega t}$. The shear stress will also be a sinusoidally varying quantity (generally with in-phase and 90° phase-shifted components) so we can write $\sigma = \sigma^*e^{i\omega t}$, where $\sigma^*$ is the complex amplitude. The governing equations are as follows, and we see that although they have a sinusoidal time dependence, they clearly have an analogous form to the elastic governing equations discussed previously ((E1) - (E4)) :

(VE1) the equation of motion (ignoring body forces and inertia effects)

$$\nabla \cdot \sigma^*e^{i\omega t} = 0 \qquad (2.6)$$

(VE2) Conservation of mass (incompressibility)

$$tr\varepsilon_0 = 0 \qquad (2.7)$$

(VE3) Constitutive equation (neglecting an arbitrary isotropic pressure)

$$\sigma(t) = \sigma^* e^{i\omega t} = \varepsilon_0 G^* e^{i\omega t} \qquad (2.8)$$

Here $G^*$ is the complex modulus of the viscoelastic material.

(VE4) The boundary conditions for the viscoelastic matrix problem are the same as for the elastic problem, since they are geometrically identical viz prescribed displacement at the probe-matrix interface $S_1$ (non-slip), and traction-free at the exposed upper surface $S_2$ (i.e. $\sigma^*.n = 0$).

In both elastic and viscoelastic contact problems, the aim is to find an expression for the instantaneous force acting on the probe : the constant force F after the step displacement in the elastic problem, and the sinusoidally varying force $F(t) = F^* e^{i\omega t}$ in the viscoelastic problem. In general, the force vector $F$ can be found by integrating the surface traction vector $\sigma.n$ over the contact interface. As seen above, the correspondence between the governing equations for the elastic and viscoelastic problems (observe the similarity between (E1) and (VE1) above, (E2) and (VE2), etc) means that the expressions for the force will also be similar, since they involve the same spatial integration of the traction vector. Thus the solution for $F(t) = F^* e^{i\omega t}$ can be obtained from the elastic solution by replacing the dependent variables by their Fourier transforms, and the material parameters by the Fourier transforms of their viscoelastic counterparts (e.g. $G$ is replaced by $G^*$, etc). See Bland (1960) for an extensive table of these "elastic-to-viscoelastic" conversions. We thus apply this principle to the general equation eq(2.2) above, enabling us to immediately write down the force signal equation for the viscoelastic case under small amplitude oscillatory displacements $W(t) = W_0 e^{i\omega t}$:

$$F(t) = F^* e^{i\omega t} = kG^* W_0 e^{i\omega t} \qquad (2.9)$$

where $F^* = F^*(\omega) = F'(\omega) + iF''(\omega)$ is the complex Fourier coefficient of the force signal $F(t)$, k is the same instrument geometry factor as in the elastic case (eq(2.2)), and $G^* = G^*(\omega) = G'(\omega) + G''(\omega)$ is the complex modulus of the sample. Often the $e^{i\omega t}$ factor is not explicitly written, leaving us with the following complex equation relating the in-phase and 90° phase-shifted components

$$F^* = kG^* W_0 \qquad (2.10)$$

Further, we point out that for the sake of concreteness we have written the displacement as $W(t) = W_0 e^{i\omega t}$ (with $W_0$ real) and the Fourier transform of this (at frequency $\omega$) is simply $W_0$. To be more general, we could let the displacement be $W(t) = W^* e^{i\omega t}$ with $W^*$ a complex number, so that the Fourier coefficient becomes $W^*$. Using this more general notation we see from eq(2.10) that the complex modulus $G^*$ is proportional to the quotient $F^*/W^*$ (a complex division) as follows

$$\frac{F^*}{W^*} = kG^* \qquad (2.11)$$

The complex quantity $F^*/W^*$, which is essentially the ratio of the "output" over the "input" is often called a "transfer function". The use of transfer functions will be discussed further in section 2.3.

It should be noted that although the previous discussion has been based on the elastic contact problem, there is an equivalent version of the correspondence principle relating Newtonian fluid response to viscoelastic response. Specifically, the principle can be employed to convert the solution to a boundary value problem involving an inertialess Newtonian liquid in steady flow, to the corresponding solution with the same geometry for a small amplitude oscillatory flow in a viscoelastic fluid. In this version of the correspondence principle, the Newtonian viscosity would be replaced by the dynamic viscosity $\eta^*(\omega) = (G''-iG')/\omega$, and the steady flow rates would be replaced by terms like $dW(t)/dt = i\omega W_0 e^{i\omega t}$. This approach is useful in deformation geometries where it is more natural to think in terms of liquids and their flows, such as in the calculation of the sliding cylinder geometry in Sect 3.3.

We conclude this introduction to the correspondence principle of linear viscoelasticity, by pointing out possible extensions of the basic principle. The effects of fluid inertia can be calculated in some special cases - see Bland (1960) for details (a brief discussion of inertia corrections is given in section 4.1). The stress relaxation response of a viscoelastic material under a step strain can also be calculated (using Laplace instead of Fourier transforms - see Bland, 1960; Tanner, 2000). Finally, it should be noted that the correspondence principle can be used to treat compressible materials (not just the case of $v = 0.5$ considered in this paper) - see Bland (1960).

## 2.2. Pseudorandom noise displacement signal and fast Fourier transforms

The above discussion has focussed on the response under a single frequency $\omega$. However, since the governing equation between force and displacement is linear (eq(2.10)), the principle of linear superposition can be invoked, meaning that we can use a more complex displacement history with a broad frequency content as the input signal. The key idea behind the superposition principle is that the force due to a series of superposed sinusoids will be the sum of the force responses that the individual sinusoids would have caused alone. Thus if a Fourier transform is carried out on the complicated displacement signal and resulting force signal, the values of the storage and loss moduli ($G^*(\omega) = G'+iG''$) at a number of different frequencies can be determined via eq(2.10). This means that with a single measurement it is possible to rapidly obtain information about the viscoelastic properties over a range of frequencies (Nelson and Dealy 1993; 1998). This is the funda-

mental approach adopted in the techniques to be discussed in this paper.

In this section we will discuss the nature and the construction of a band-limited pseudorandom noise signal, which is used as the input strain signal in the different probe geometries described in Sect. 3. We will also discuss algorithms such as the Fast Fourier Transform which enable efficient conversion of the time dependent force response signal to the frequency domain.

To begin, let us consider the general Fourier series for a function $F(t)$, which is assumed to be periodic with period $T$. We assume that $F(t)$ is represented by a series of $N$ discrete data points, measured at equal time intervals. For a series of data points such as this, the Discrete Fourier Transform (DFT) is used to separate the waveform into the Fourier components. The DFT calculates the complex amplitudes at each of the discrete frequencies that make up the Fourier series representation of the discrete signal. That is, the DFT determines the coefficients $a_j$ and $b_j$ in the following Fourier series:

$$F(t) = \sum_{j=0}^{N-1} a_j \cos(\omega_j t) + b_j \sin(\omega_j t) \tag{2.12}$$

Here $\omega_j$ are integral multiples of the fundamental frequency $\omega_0 = 2\pi/T$. The coefficients $a_j$ and $b_j$ are real numbers. We will find it convenient to incorporate $a_j$, $b_j$ into the complex quantity $F^*(j)$, and write more compactly (Bracewell, 2000)

$$F(n) = \sum_{j=0}^{N-1} F^*(j) \exp(i2\pi jn/N) \tag{2.13}$$

Here $n$ is an index referring to the data point series. $F^*(j)$ is the discrete, complex-valued frequency domain series, and can be calculated from $F(n)$ as follows:

$$F^*(j) = \frac{1}{N} \sum_{n=0}^{N-1} F(n) \exp(-i2\pi jn/N) \tag{2.14}$$

The above equation is the Discrete Fourier Transform of the series of data points describing the function $F(t)$ (or equivalently $F(n)$). We see that since the Fourier transform is linear, a sinusoidal component added in the time domain will also be added to the same proportion in the frequency domain. Thus, it is possible to construct a waveform with a desired frequency spectrum by adding together appropriate waveforms in the time domain : that is, components from each waveform are added until the sought-for frequency spectrum is achieved. In this review, we focus on displacement waveforms which are band-limited pseudorandom excitation sequences. These have similar autocorrelations as white noise (i.e. a single impulse at lag 0) but are cyclic, so that ideally only one period of the waveform need be sampled to obtain all necessary information, and they usually have a flat frequency spectrum although this can be adjusted if necessary. The frequency range and res-

olution are controlled by the number of discrete data points $N$ and the interval length $\Delta t$ in the time domain. Pseudorandom noise signals are often used as the input signal in various electronic circuits etc to estimate the linear response behaviour as a function of excitation frequency (see e.g. Horowitz and Hill, 1989)

There are several ways to generate a pseudorandom noise signal. Pseudorandom binary sequences PRBS, also called "binary maximum length sequences (BMLS)", have been developed for use in rheological applications (Nelson et al., 1994; Nelson and Dealy, 1998). Basically PRBS's consist of a series of steps between two signal levels, with the level changed only at certain discrete time intervals. The result is a sequence of chains of ON or OFF states of different duration, and this is the strain time pattern imposed on the sample. Nelson and Dealy (1998) describe measurements performed on a silicone putty (polydimethylsiloxane) in a rotational rheometer using the arbitrary waveform option and an external waveform generator producing a PRBS sequence consisting of 1240 points. Fourier analysis was carried out on the resulting torque signal and it was found that the technique was able to measure the viscoelastic properties of the sample over the frequency range applied. Nelson and Dealy focussed on the lower frequency behaviour, with a bandwidth of 0.06-0.6 Hz. Another possible pseudorandom sequence is the randomly switched bi-level waveform, which resembles the PRBS but is based on a different algorithm whereby at each instant of time the signal switches to the opposite state with a given probability.

An alternative method of producing band-limited pseudorandom noise displacement signals, and indeed the method used in the tests described in section 3, is to notice that the Fourier representation of a time signal $F(t)$ can also be written as $F(t) = \sum_{j=0}^{N-1} A_j \cos(\omega_j t + \delta_j)$ where $A_j$ is a real constant and $\delta_j$ is the phase angle. Here, for each frequency component (i.e. each $\omega_j$), the amplitude $A_j$ is set to a predetermined mean value and simultaneously the phase angle $\delta_j$ is varied randomly between 0 and $2\pi$. Using this approach, the band-limited pseudorandom noise signal can be synthetically generated and then stored in the instrument's operating program. More details about the characteristics of pseudorandom noise and some digital circuits which can be used for their generation can be found in, for example, Horowitz and Hill (1989). In addition to the pseudorandom signal, another technique which can be useful for spectral analysis is the CHIRP/Z transform (Horowitz and Hill, 1989), where the signal is a linear scan of frequency versus time for each sweep, with the response signals from the entire band of frequencies being gathered continuously.

Once the pseudorandom strain signal has been applied to the sample and the resistance force signal is recorded, the Fourier transform is applied to the force waveform $F(t)$ in the time domain to convert it to the frequency domain.

Although the formula presented in eq(2.14) could be used directly (i.e. numerically solve for $F^*(j)$ for each $j =$ 0,1,2,..., $N$-1) this calculation can be quite lengthy if there are many data points - indeed for $N$ data points the time required would be proportional to $N^2$. These days, the most common procedure is to use the Fast Fourier Transform (FFT) as developed by Cooley and Tukey (1965), which greatly accelerates the calculation (with this algorithm the calculation length scales as $N \log_2 N$). These FFTs are often available as commercial software packages, and for details of the programming algorithm, the reader is referred to the many books now available on the subject (e.g. Ramirez, 1985; van Loan, 1992; Walker, 1996). For our purposes in this review, it will suffice to note that the FFT is a highly efficient way to extract the Fourier components of the time signal, and will give us the sought-for function $F^*(\omega) = F'(\omega) + iF''(\omega)$.

Although we will skip over the details of the Fast Fourier Transform, it would be useful to point out some general issues which need to be considered when implementing these pseudorandom noise signals together with the FFT algorithm. These issues will be listed here and briefly described, and the interested reader is urged to consult the original references for further details:

(a) The sampling rate, which is the rate at which the data points are being measured during an experiment, is a key quantity. If we write $f_s$ for the sampling frequency, Shannon's theorem (also known as the Nyquist sampling theorem - Bracewell, 2000) states that $f_s$ must be at least twice the highest frequency component in the sample being measured, which for this discussion we will write as $f_{max}$. If the sampling rate is too low, the problem of "aliasing" may occur, which is the apparent association of higher frequency components with an incorrect lower frequency, brought about by the fact that the sampling rate is unable to keep track of the rapid changes of the high frequency components of the signal. Aliasing affects both the magnitude and phase of the signals. It is important to be aware of this aliasing possibility even if the sampling rate is well above the upper limit of the bandwidth of interest, since if the signal used has significant higher harmonics above the upper limit frequency, these will be aliased into the lower frequencies of interest and contaminate the results. In fact, the waveform is often passed through a filter so that higher frequency harmonics are removed. On the other hand, too high a sampling rate will lead to the collection of surplus data, with excessive data storage requirements and long calculation times.

(b) Care needs to be taken when setting the data acquisition conditions for an experiment (i.e. the sampling rate and the number of data points $N$ in the time domain series). Particularly, it is essential that an integral number of cycles be sampled for each frequency, since this ensures that the frequency components of the signal will fall exactly on the

corresponding discrete points in the Discretised Fourier Transform. If the sampling conditions are such that a non-integral number of waveforms are sampled, a phenomenon called "leakage" can occur (e.g. see Ramirez, 1985; Nelson and Dealy, 1998; Bracewell, 2000) which results in incorrect amplitudes and phases being attributed to the frequency nodes. Leakage is also expected to occur if truncated data strings are used (Bracewell, 2000). We point out that there are special "windowing" techniques which can be employed to reduce problems due to leakage if non-periodic samples are to be sampled (e.g. Ramirez, 1985).

(c) While greatly accelerating the computation of the discrete Fourier transform (eq(2.14)) the Fast Fourier Transform has the limitation that it generally requires the number of data points in the time series to be of the form $2^m$ (i.e. have 2,4,8,16, .... data points) (Bracewell, 2000). Versions of the FFT have been developed which can handle an arbitrary number of data points in the time series, such as using data string lengths of $3^m$, $5^m$, $7^m$ etc or adding zeros to the data string to extend the data to $2^m$ elements (see Bracewell, 2000). However care should be taken to ensure that no artefacts appear in the frequency spectrum data due to these procedures. Many of these techniques have been built into recent commercial software packages such as MATLAB (version 3.5) whose $fft()$ function will accept any number of data points.

(d) The measurements of the force signal should be commenced after start-up transient behaviour becomes negligible, usually after several excitation cycles have been imposed (Nelson and Dealy, 1998). The length of time required before the start-up transients can be neglected for a particular sample can be estimated from stress relaxation tests.

(e) It should be confirmed that with the data acquisition systems used, the stress and strain signals are sampled at precisely the same moment, otherwise an extra phase shift may be introduced between stress and strain which affects the calculated value of the rheological phase shift $\delta$. If the method of data acquisition is known (e.g. alternate sampling from the two channels), it is possible to approximately correct for the extra phase shift introduced (Nelson and Dealy, 1998). Further, care in this regard should also be taken when using electronic filters to improve the quality of data acquired (e.g. anti-aliasing filters which are low pass filters with high frequency cutoffs), since these can also affect the phase difference between the stress and strain signals.

(f) The signal-to-noise ratio can be increased by sampling over a large number of displacement sequences. Nelson and Dealy (1998) recommend that the average of the data points be taken in the time domain first, and then the Fourier transform be applied to this averaged time domain data series. Although it is possible to take Fourier transforms of each cycle individually and calculate the average

of these, computations performed this way can be become quite long.

(g) To characterise the nature of the response in the frequency domain, a "power spectrum" is often used, defined generally for a function $H(t) = H^*e^{i\omega t}$ by $G_{HH}(\omega) = |H^*(\omega)|^2$. In the experiments described in section 3, the average power spectrum calculated over several cycles of the displacement signal is typically quite flat over the range of frequencies of interest (typically 1 Hz to 100 Hz). However, it should be noted that a flat power spectrum for the displacement means that the forces corresponding to the higher frequency components may be large, since the shear rate amplitude is highest for those frequencies ($\propto \omega\gamma_0$ with $\gamma_0$ essentially constant). It is possible to use displacement signals where the power spectrum decreases at higher frequencies to compensate for this effect (Field, 1995).

### 2.3. Determination of the viscoelastic properties using transfer functions

Once Fourier transforms have converted the displacement signal and force signal data to the frequency domain giving us $W^*(\omega)$ and $F^*(\omega)$, the final step is to obtain the frequency-dependent viscoelastic properties $G^*(\omega)$ using the force-displacement relation eq(2.10). The ratio of output over input in the frequency domain (here, $F^*/W^*$-eq(2.11) is often called a "transfer function" (TF), which is a complex number and a function of frequency $\omega$.

Transfer functions are commonly used since they efficiently facilitate a process called "frequency domain equalization" which is often carried out to improve the data quality (Horowitz and Hill, 1989). In the rheological tests described here (Sect. 3), it is inevitable that the measured quantities become convoluted with the imperfect response of the instrument itself (also a function of frequency) and correction for this in the time domain is practically impossible. However, convolution of the data in the time domain becomes a straightforward product in the frequency domain, and correction is relatively simple, ie the measured transfer function can be written as the product $TF_{sample} \cdot TF_{instrument}$, where $TF_{sample}$ is the idealised transfer function for the material in the absence of any instrument contamination, and $TF_{instrument}$ describes the instrument's frequency dependent behavior. The procedure involves writing $TF_{sample}$ as follows

$$TF_{sample}(\omega) = TF_{ref} \frac{TF_{sample} \, TF_{instrument}}{TF_{ref} \, TF_{instrument}} \qquad (2.15)$$

where $TF_{ref}$ is the (deconvoluted) transfer function for a reference material with known mechanical properties, determined by a separate independent measurement. Field and co-workers (Field, 1995; Field et al., 1996) describe the use of linear springs of known stiffness (where $TF_{ref} = k$, the spring constant) or Newtonian fluids with a known viscosity $\eta$ ($TF_{ref} = i\omega\eta$). The software for the oscillatory

squeeze flow instrument (section 3.1) incorporates frequency domain equalization. Eq.(2.15) clearly demonstrates the advantage of introducing the response of the reference material, since the non-convoluted transfer function for the sample $TF_{sample}$ can be obtained by complex division of the two measured functions, multiplied by a known non-convoluted function $TF_{ref}$. Thus we see that with this procedure, it is not necessary to separately determine the instrument response $TF_{instrument}$.

## 3. Applications in different rheometer geometries

### 3.1. Oscillatory squeeze flow

As illustrated in Fig. 2, in this geometry the film-like sample is sandwiched between two parallel circular plates. The upper plate is oscillated vertically about a mean position with a small amplitude, and since the sample maintains adhesion with both plate surfaces, oscillatory squeeze flow is induced. The force exerted by the sample on the stationary bottom plate is detected by the load cell directly underneath. Typically the motion used is a band-limited pseudorandom noise signal with frequency range of 3 Hz to 100 Hz. Fourier analysis is carried out on the force signal to extract the viscoelastic properties, as discussed in Section 2. The development of this instrument, called the "Micro-Fourier Rheometer" was a joint project between the University of Sydney and the Commonwealth Scientific and Industrial Research Organisation (Field, 1995; Field et al., 1996; Phan-Thien et al., 1996), and currently efforts are being made toward commercialisation.

Presently there is an extensive body of literature on the use of squeeze flow for rheological characterisation of materials. There have been many studies of the response of materials in squeeze flow under constant compressive force, or constant squeezing speed : the reader is referred to the reviews in Bird et al. (1987), Macosko (1994), Gibson et al. (1998), Tanner (2000) and references therein. Introducing a very thin lubricating film between the plate surfaces and the sample leads to biaxial extensional flow, and this has also been studied by several workers (reviewed in Macosko, 1994). However, there appear to be no reports of the use of small amplitude oscillatory squeeze flow to characterise the viscoelastic properties of thin-film samples, which will be the focus of the rest of this sub-section.

We consider a sample undergoing small amplitude oscillatory squeeze flow, and seek the governing equation relating the force signal $F(t) = F^*e^{i\omega t}$ to the upper plate motion $W(t) = W_0e^{i\omega t}$. The first step is to write the instantaneous resistance force $F$ for a thin film of Newtonian liquid of viscosity $\eta$ when the upper plate is moved down with a velocity $V$ with the bottom plate stationary. We ignore inertia effects and use the thin film lubrication approximation (valid if the ratio of the upper plate diameter to film thick-

ness is at least 10:1) and obtain the following well known Stefan equation (see e.g. Bird *et al.*, 1987):

$$F = k_{squeeze}\eta V \qquad (3.1)$$

Here $k_{squeeze}$ depends on the radius $a$ and the sample thickness $h_0$, and is given by

$$k_{squeeze} = \frac{3}{2}\frac{\pi a^4 \eta}{h_0^3} \qquad (3.2)$$

Following the discussion in section 2.1, the next step is to convert this Newtonian liquid result via the correspondence principle to a formula for a viscoelastic fluid sample where the upper plate undergoes small amplitude oscillatory displacements $W(t) = W_0 e^{i\omega t}$ about the mean position shown in Figure 2. A key assumption is that throughout the oscillatory displacements, the fluid remains adhered to the plates. A simple substitution into eq(3.1) (Field *et al.*, 1996) will yield the sought-for instantaneous force which will be a sinusoid $F(t) = F^*e^{i\omega t}$ with $F^*$ given by

$$F^* = k_{squeeze}G^*W_0 \qquad (3.3)$$

where $k_{squeeze}$ is the same instrument geometry factor eq(3.2), and the complex modulus $G^* = G'+iG''$. Eq(3.3) is the governing equation for the oscillatory squeeze flow technique and we see that it indeed has the general form discussed in section 2.1 (eq(2.10)). Note that from eq(3.3) we find that the transfer function $TF = F^*/W^* = F^*/W_0$ (section 2.3) becomes

$$TF = k_{squeeze}G^* \qquad (3.4)$$

Referring to Fig. 2, we now describe the experimental set up. The upper plate was made of polished stainless steel with the radius $a$ typically 15 mm, and was attached to a vertical motion driver which in turn was connected to a signal generator with feedback. The driver was made from
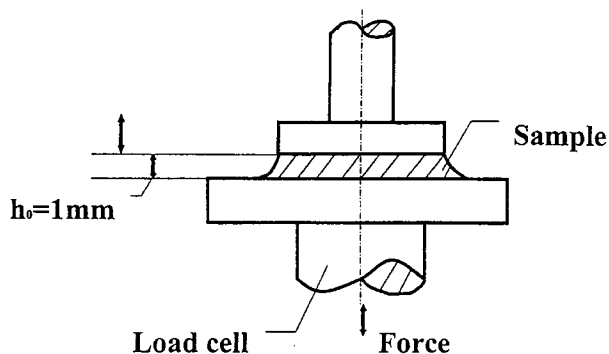


**Fig. 2.** A schematic representation of the oscillatory squeeze flow test (section 3.1). The stationary bottom plate is attached to a load cell, and the upper plate is oscillated vertically with a small amplitude $W(t) = W_0 e^{i\omega t}$ with $W_0/h_0 \ll 1$.

Terfenol-D, a giant-magnetostrictive rare earth material which undergoes large strains with the application of a moderate external magnetic field (Goodfriend, 1991), and was purchased from ETREMA Products, Inc. (USA). To ensure symmetric motion, the driver was preloaded mechanically (with a spring) and magnetically (with a permanent magnet), and the variational magnetic field was produced by a coil operating at low voltage and moderate current. The output motion (up to 100 Hz) was linearised using a PID feedback controller. The instantaneous vertical position of the upper plate was detected by a fibre-optic device, giving the displacement $W(t)$. The amplitudes of the oscillatory motions were kept small, typically less than 5 $\mu$m, and the mean gap value was 1 mm. The bottom plate remained stationary, and a piezoelectric load cell rigidly attached underneath was used to measure the instantaneous force $F(t)$. Analog signals from the load cell are digitised using analog to digital convertors (ADC). These were synchronised with the signals from the position detection system and the digital values were used by the computer software to calculate the discrete Fourier transforms. Overall, the instrument is constructed to have a very high stiffness with a resonance frequency well above the operating frequency range (see the discussion in Field, 1995).

As discussed in Section 2.3, frequency domain equalization was carried out on the transfer function to correct for imperfections of the instrument response. As a reference material, a small compression spring of known spring constant was used, although equivalently a Newtonian fluid of known viscosity could also be used (Field *et al.*, 1996).

Measurements of the linear viscoelastic properties of several types of materials have been successfully carried out using this instrument : standard Newtonian oils and synovial fluids (Field, 1995; Field *et al.*, 1996), bitumens (Swain *et al.*, 1997), concentrated suspensions of particles dispersed in oils and polymer solutions (See *et al.*, 1998; See *et al.*, 2000b; see Fig. 3). The oscillatory squeeze flow instrument with pseudorandom noise displacements has also been used to monitor the setting behaviour of alginate-based dental materials (Gonsalkorale *et al.*, 1999). In all of these tests, an important step prior to the use of the pseudorandom noise displacement signal was the confirmation that the material was responding in the linear viscoelastic regime. This was checked by applying a single frequency input signal for the upper plate motion, and observing that the force signal was indeed sinusoidal, with an amplitude proportional to the displacement amplitude. For the majority of the samples, comparative tests were also made with conventional rheometers (e.g. cone-plate, parallel plates) and there was good agreement observed for the values of $G'$ and $G''$ obtained with the pseudorandom squeeze flow. Finally, as will be discussed in section 4.1, fluid inertia can affect measurements of a material's response in oscillatory flows, particularly the values of $G'$, and for oscillatory
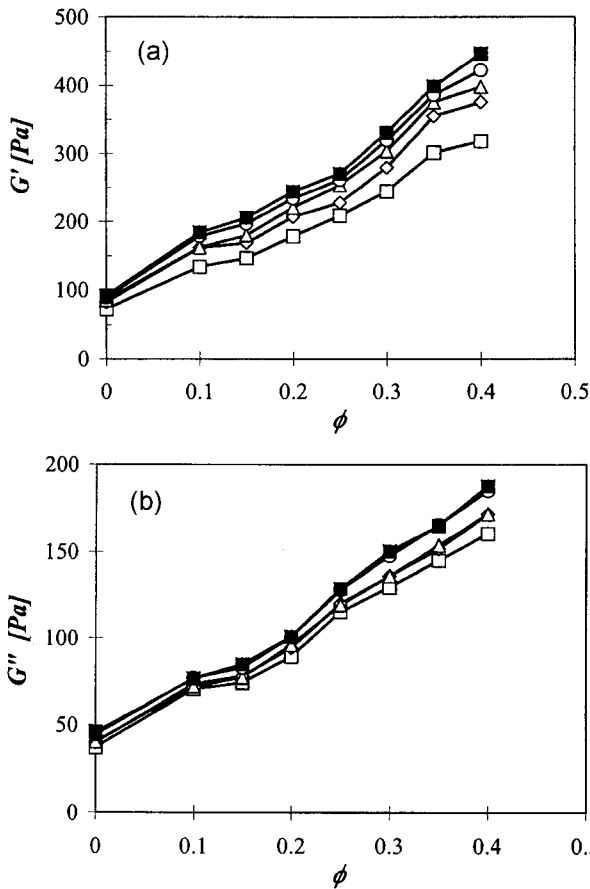
**Fig. 4.** A schematic representation of the oscillating imbedded needle experiment (section 3.2).

**Fig. 3.** Linear viscoelastic properties of suspensions of polyethylene particles with average diameter 80 $\mu$m dispersed in 3% by weight Separan polymer solution, as a function of particle volume fraction $\phi$, measured by the pseudorandom noise and the oscillatory squeeze flow method (See et al., 2000b). (a) The storage modulus $G'$ and (b) loss modulus $G''$ are plotted as functions of $\phi$ and oscillation frequency ($\square$ 20 Hz, $\diamondsuit$ 40 Hz, $\triangle$ 60 Hz, $\bigcirc$ 80 Hz, $\blacksquare$ 100 Hz).

squeeze flow a theoretical treatment of this problem has been presented by Phan-Thien et al. (1996). These workers derived a correction formula for $G'$ which has in fact been incorporated in the instrument's operating software.

The rapidity of the tests achieved by the use of pseudorandom noise signals is an attractive feature, and indeed the tests using this technique were carried out in a time significantly less than the time required to measure individually at each frequency over the same frequency range. Typically, a measurement over one cycle of the pseudorandom strain series will take slightly longer than the period of the lowest frequency sampled.

Finally, we point out that, as shown by Field (1995), the dominant contribution to the resistance force is the thin fluid film sandwiched under the upper plate, and for most materials there is negligible effect from the meniscus or
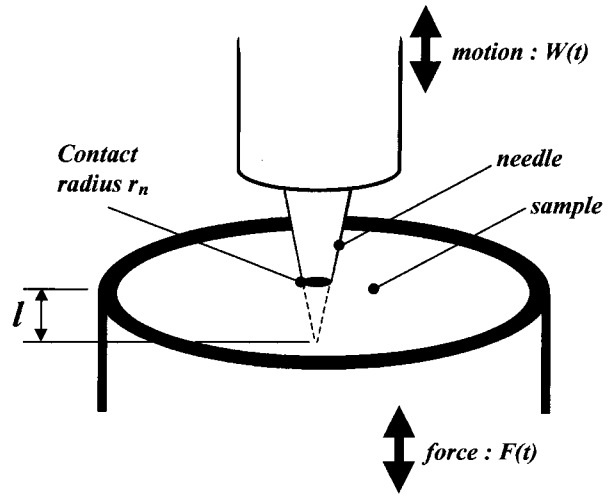
indeed any of the surrounding material beyond the radius of the upper plate. Hence it may be possible to test samples that are considerably spread out beyond the edge of the upper plate, suggesting that this method could find use in a more portable device for testing film-like samples (e.g. as an on-line tester in sheet production processes).

### 3.2. Oscillating imbedded needle

As illustrated in Fig. 4, this geometry uses a slender needle which is imbedded normally into the sample surface, and made to oscillate axially with a small amplitude about this position. The instantaneous force $F(t)$ acting on the sample vessel is detected by a load cell (this equals the force acting on the needle since inertial effects are negligible). The dynamic viscoelastic properties of the sample can thus be determined using pseudorandom displacement signals and Fourier analysis (See et al., 1999b).

There have been some previous instruments which used a similar basic approach of an oscillating imbedded probe. Particularly noteworthy are the Vibrating Needle Curemeter (VNC) developed by the Rubber and Plastic Research Association (Pethrick, 1993; Pethrick, 1998), and the vibrating paddle rheometer (Affrossman et al., 1990; Banfill et al., 1991; Radhakrishnan and Pethrick, 1994; Pethrick, 1993; 1998). The VNC worked on the principle of a needle attached to a moving electromagnetic coil which was located close to one pole of a permanent magnet. An AC current energised the coil which vibrated the needle at the AC frequency, usually chosen to be close to the resonance frequency of the assembly. The reduction in oscillation amplitude when the needle was placed in a sample was detected as a change in the back EMF in the coil, enabling the degree of viscosity of the sample to be determined. The VNC was chiefly developed for the purpose of monitoring the curing process in reactive chem-

ical systems. The vibrating paddle rheometer follows the same principle but with a small paddle immersed in the sample, and used more sophisticated position sensing via a linear variable differential transformer, enabling the in-phase and 90 phase-shifted components of the response to be determined (proportional to $G'$ and $G''$). This instrument has an interesting history : it was developed from the 1980's in a collaborative project between Strathclyde University (Prof. Pethrick) and the Carter Baker Enterprises Ltd company. It was first marketed as the "Strathclyde Rheometer", and when the company was taken over by Polymer Laboratories Ltd, the instrument name was changed to the Thermal Scanning Rheometer (the name reflecting the system's ability to apply thermal ramping to samples during the mechanical tests). Subsequently the materials testing division of Polymer Laboratories was acquired by Rheometrics Inc. (later Rheometric Scientific Inc.). Both the VNC and vibrating paddle systems used single frequency small amplitude sinusoidal oscillations at any one time. With these data the viscoelastic properties of the sample could be extracted, although calibration of the instruments with a standard sample of known viscoelastic properties was required. A first principles theoretical derivation of the force-displacement relation does not seem to be available for these instruments. The interested reader is encouraged to see the detailed review by Pethrick (1998) and references therein, for further information on the Vibrating Needle Curemeter and the vibrating paddle instrument.

Recently the use of the imbedded oscillating needle technique combined with a pseudorandom noise displacement signal and Fourier analysis has been reported by See et al. (1999b). These experiments have some parallels to the oscillatory squeezing flow method above (section 3.1) : the Terfenol-D driver was directly attached to the needle, and the sample was held in a vessel rigidly attached to the piezoelectric load cell underneath. Typical dimensions were (referring to Fig. 4): $l = 2$ mm, $r_n = 0.25$ mm. The sample vessel was typically 7 mm in radius and 9 mm deep. The oscillation amplitudes were typically less than $2 \mu$m.

We require the governing equation relating the instantaneous resistance force $F(t)$ to the needle motion $W(t)$. The calculation process involves using the slender body theory and replacing the needle by a line distribution of "Mindlin states", which are the stress and strain distributions induced by a point force acting near the free surface of an elastic halfspace (for other calculations of this kind see e.g. Russel, 1973; Phan-Thien and Goh, 1981; Phan-Thien et al., 1982; Phan-Thien and Kim, 1994). The interested reader is referred to See et al. (1999b) for details of the calculation for the elastic matrix, but the final result is that the force $F$, after a small strain $W$ has been applied to the needle, is given by the following:

$$F = k_{needle} G W \tag{3.5}$$

Here $G$ is the shear modulus of the matrix, and $k_{needle}$ is a constant determined by the needle geometry, which approaches the asymptotic value of $2l\pi[\ln(2l/r_n)]^{-1}$ as the aspect ratio $l/r_n \rightarrow \infty$. For needles of finite thickness, $f_{needle}$ has been calculated numerically by a boundary element method assuming different needle shapes - detailed results have been graphed and tabulated in See et al. (1999b).

We now use the correspondence principle of linear viscoelasticity to extend this result for an elastic matrix to yield the formula for the instantaneous force $F(t) = F^* e^{i\omega t}$ when the matrix is viscoelastic and the needle is undergoing small amplitude oscillations $W(t) = W_0 e^{i\omega t}$ about the mean imbedded depth $l$. The governing equation will thus take the form

$$F^* = k_{needle} G^* W_0 \tag{3.6}$$

where $k_{needle}$ is the same as above and $G^*$ is the complex modulus.

Eq(3.6) is the governing equation for the imbedded needle method, and we see that it does have the general form of eq(2.10). Thus with this method as well, band-limited pseudorandom noise can be used as the input displacement signal to obtain the frequency dependent material properties from Fourier analysis of the force signal $F(t)$.

A series of experiments using this technique to measure the linear viscoelastic properties of bituminous materials have been reported (Swain et al., 1997; See et al., 1999b; See et al., 2000a). In these tests the force-displacement relation eq(3.6) was used directly without any frequency domain equalisation, but reasonable agreement was observed between results obtained with this technique and those obtained independently using the parallel plate configuration. The frequency range explored with the pseudorandom noise input signal was 2 Hz to 50 Hz. Typical data curves are shown in Fig. 5. It should be noted that for these high viscosity materials, the effects of surface tension are not large. Further, tests with different sized sample vessels and needle positions showed that the walls and bottom of the chamber had a minimal effect on the measurement results, provided the needle was inserted at least 3 mm from a wall and the imbedded depth was less than 3 mm.

### 3.3. Concentric sliding cylinders

As illustrated in Fig. 6, this geometry uses a pair of concentric cylinders, with the hollow inner cylinder being slid axially through the outer fixed cylinder with no relative torsional motion (See, 2000). A pseudorandom noise displacement is used for the motion, and the force $F(t)$ acting on the outer cylinder and sample vessel are detected, enabling determination of the dynamic viscoelastic prop-
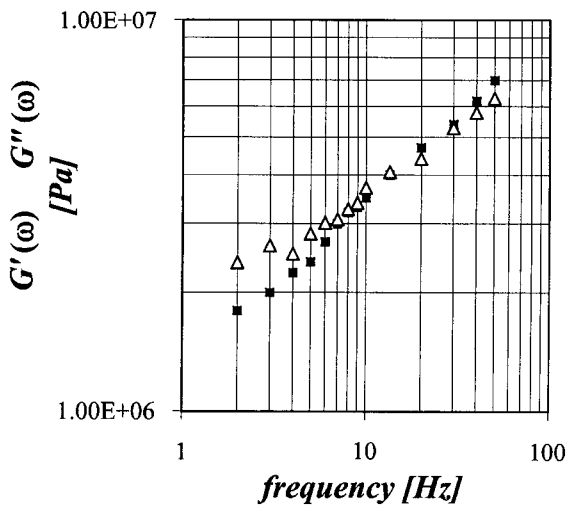
**Fig. 5.** The storage modulus $G'$(■) and loss modulus $G''$ ($\triangle$) versus oscillation frequency ($f = \omega/2\pi$) of a polymer-modified bitumen obtained with pseudorandom noise and the oscillatory imbedded needle method.
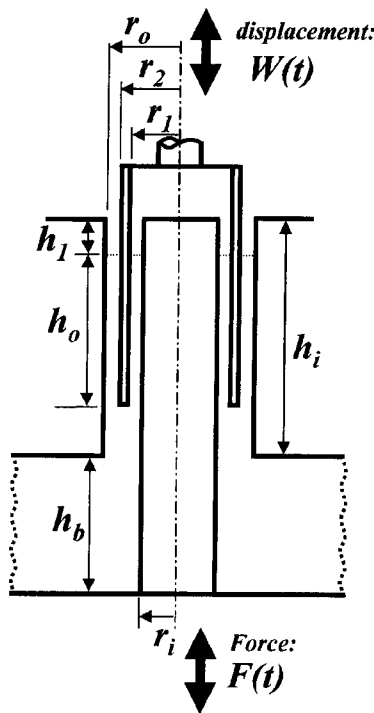


**Fig. 6.** A schematic diagram of the concentric cylinder apparatus (section 3.3). The inner cylinder slides through the sample and the outer fixed cylinder, which is fixed to an acrylic vessel (outermost boundaries omitted for clarity).

erties of the fluid which occupies the annulus between the cylinders.

Similar geometries have been reported for measurements of steady viscosity etc, and several reviews of these works are available (Oka, 1960; Bird *et al.*, 1987; Whorlow, 1992;

Dealy and Giacomin, 1998). Particularly noteworthy in the context of the oscillatory methods discussed in this paper are experiments which have used axially oscillated concentric cylinders : Bikerman (1948) who measured viscosity of solutions of rosin in turpentine and rosin in benzyl benzoate, and Smith *et al.* (1949) who examined solutions of polyvinyl acetate in cyclohexane and polyisobutylene in xylene. More recent reports using this deformation geometry include Hibberd and Parker (1975) who studied the viscoelastic properties of bread doughs, McCarthy (1978) on polymer melts, and Tsai and Soong (1985) on concentrated polymer solutions. These previous works have all used single frequency sinusoids for the input displacement of one of the cylinders, and most used a solid inner cylinder.

See (2000) used the pseudorandom noise technique, and a hollow inner cylinder to increase the "wetted" surface area and hence the force sensitivity. The experimental set-up parallels that of the oscillatory squeezing flow and imbedded needle configurations, described previously. The Terfenol-D driver was centrally attached to the top of the brass inner cylinder, and the brass outer cylinder and acrylic sample vessel were rigidly fixed to the piezoelectric load cell underneath. Referring to Fig. 6, the dimensions are (all lengths in mm): $r_i = 2.5$, $r_1 = 3.0$, $r_2 = 3.5$, $r_0 = 4.0$, $h_0 = 8.0$, $h_i = 13.0$, $h_b = 7.2$, $h_1 = 1.9$.

As with the previous two geometries, we require the governing equation relating the instantaneous resistance force $F(t)$ to the inner cylinder motion $W(t)$. The detailed calculations can be found in See (2000), but the first step is to find the equation relating the force $F$ to the instantaneous downward velocity $V$ of the inner cylinder when a Newtonian liquid is used. Assuming laminar flow and ignoring fluid inertia, fluid dynamics calculations give us (See, 2000):

$$F = k_{conc}\eta V \tag{3.7}$$

Here $\eta$ is the Newtonian viscosity, and $k_{conc}$ is an instrument geometry factor defined as follows:

$$k_{conc} = 2\pi h_0[2f^2/g + 1/\ln R_0 + 1/\ln (R_1/R_i)] \tag{3.8}$$

with

$$f = \frac{(R_0^2 - 1)}{\ln R_0} - \frac{(R_1^2 - R_i^2)}{\ln\left(\frac{R_1}{R_i}\right)} \tag{3.9}$$

and

$$g = (R_0^2 - 1)\left\{R_0^2 + 1 - \frac{R_0^2 - 1}{\ln R_0}\right\} + (R_1^2 - R_i^2)\left\{R_i^2 + R_1^2 - \frac{(R_1^2 - R_i^2)}{\ln\left(\frac{R_1}{R_i}\right)}\right\} \tag{3.10}$$

We have used here $R_0 = r_0/r_2$, $R_1 = r_1/r_2$ and $R_i = r_i/r_2$.

The correspondence principle allows us to convert this Newtonian liquid result to one for a viscoelastic fluid undergoing small amplitude oscillatory displacements $W(t) = W_0 e^{i\omega t}$ about the position shown in Fig. 6. The instantaneous force will thus also be a sinusoid $F(t) = F^* e^{i\omega t}$ with $F^*$ given by

$$F^* = k_{conc} G^* W_0 \qquad (3.11)$$

where $k_{conc}$ is given by eq(3.8). We see again that this equation is of the general form eq(2.10), meaning that band-limited pseudorandom noise can be used as the input displacement signal with Fourier analysis of the force signal to give the frequency dependent material properties.

A series of experiments was carried out employing this concentric cylinder configuration with pseudorandom noise, using high viscosity silicone oils with different molecular weights (See, 2000). In these tests the equation was used directly without any frequency domain equalization, but similar to the imbedded needle case in Section 3.2, reasonable agreement was observed between the material properties found by this method and those obtained with the parallel plate configuration.

### 3.4. Other geometries

As the above applications show, provided the force-displacement relation is known (the general relation eq(2.10)), a wide range of deformation geometries can in principal be used to determine linear viscoelastic properties. Further, the linear nature of these relations permits the use of a band-limited pseudorandom noise excitation sequence for the displacement signal, with Fourier analysis of the force signal giving the frequency dependent viscoelastic properties. For any deformation geometry, key assumptions are that the sample maintains adhesion throughout the motion cycle, and that the displacement amplitudes are small compared to other instrument length scales.

Other deformation geometries include the imbedded paddle geometry of the Strathclyde curemeter, as discussed in section 3.2. A similar approach was adopted by Shikata *et al.* (1997) who oscillated small glass plates inserted normally into liquid-like samples to determine the viscosity. There are numerous non-conventional rheometer geometries which have been originally designed for measurements of steady viscosity, but which could be used for determination of viscoelastic properties if the force-displacement relation (eq(2.10)) is available (e.g. rheometers based on parallel sliding plates, etc; see reviews by Mackay, 1993; 1998).

There is an extensive body of literature on elastic contact problems - see for example, the books by Johnson (1987) and Hills *et al.* (1993). Provided that the relationship between displacement and force is linear and the boundary conditions do not change fundamentally with the indentation (as discussed in Pipkin, 1986), we can use these elastic results via the correspondence principle to obtain the force-displacement equations for the corresponding oscillatory contact problems on a viscoelastic halfspace. For example, Pipkin (1986) discusses the case of a flat-headed circular punch (radius $R$) pressed normally onto a halfspace with displacement $W_0$. As discussed in Johnson (1987) it is possible to mathematically account for the infinite pressure located right at the edges of the sharp square corners in this problem. Pipkin (1986) showed that, in general, the force $F$ can be written $F = Rg(v)GW_0$ where the function $g(v)$ is a pure number depending on Poisson's ratio $v$ (Pipkin, 1986). For the same punch undergoing small amplitude oscillations on the viscoelastic halfspace, the governing formula becomes $F^* = RgG^* W_0$ (letting $v = 1/2$ - Pipkin, 1986).

Finally, we point out that up to now all the probes presented in this paper have been oscillated normally to the sample surface, but in fact the oscillations could be applied at an angle to the interface. For example, small amplitude oscillations could be applied at the contacting area tangentially to the surface and, provided that the sample adheres to the probe surface and that the linear force-displacement relation can be determined (eq(2.10)), an instrument operating in this mode could in principle be used to measure viscoelastic properties.

## 4. Other issues

### 4.1. Inertia effects

It is well known that in any rheometer design where the samples are placed under oscillatory strains, fluid inertia effects can arise (Walters, 1975; Ferry, 1980; Whorlow, 1992). The effect is more pronounced for lower viscosity fluids at high oscillation frequencies (e.g. Field *et al.*, 1996; Phan-Thien *et al.*, 1996). The contribution of fluid inertia to the measured force response is essentially a (mass)×(acceleration) term resulting from the fluid motion, and will act in anti-phase to $G'$ thus reducing the measured value of this quantity. The reduction in $G'(\omega)$ due to fluid inertia is proportional to $-\rho\omega^2$, where $\rho$ is the density of the fluid, and the numerical prefactor needs to be calculated from first principles for each flow geometry. Theoretically $G''$ is unaffected by inertial effects.

For the oscillatory squeeze flow discussed in section 3.1, an inertia correction for $G'$ has been theoretically derived from first principles by Phan-Thien *et al.* (1996). These workers carried out small strain analysis and asymptotic expansions based on the Stokes number, and found that $G'$ was reduced by the following amount $\Delta G'$:

$$\Delta G'(\omega) = \frac{1}{10} \rho h_0^2 \omega^2 \qquad (4.1)$$

## 4.2. Larger amplitudes and non-linear viscoelasticity

With any of the devices discussed in section 3, under large strain amplitudes the response may no longer be in the linear viscoelastic regime. It is sometimes useful to deliberately apply large amplitude displacements in order to find the critical strain for linear viscoelasticity, as well as to illuminate features of the response under large deformations. For example, using the oscillatory squeeze flow instrument (Sect. 3.1) with a single frequency excitation, See and co-workers (See et al., 1997; See et al., 1999a) have studied the response of a yield stress material (electrorheological fluid under high electric field), and observed that the yielding behaviour is clearly manifested in the non-harmonic shape of the force signal. Other works which have used large amplitude oscillatory squeeze flow include Phan-Thien et al. (2000) who examined the non-linear behaviour of biological tissue (amplitudes up to 20 $\mu$m using a 1 mm gap), and Jiang et al. (2001) who monitored the change from linear to non-linear viscoelastic behaviour at fixed strain amplitude during the setting of a dental composite cement. It should be noted that the pseudorandom noise signal cannot be employed in these tests since the principle of linear superposition does not hold for non-harmonic behaviour, and hence single frequency sinusoids were used (usually at 10 Hz or 20 Hz). It should also be pointed out that some care is needed in interpreting the results since most of these geometries do not impose spatially uniform strain fields to the sample. Thus these tests are more of a qualitative indication as to the onset and degree of non-linear viscoelastic behaviour.

## 5. Conclusions

This paper presents an overview of recent developments in the use of band-limited pseudorandom noise strain signals with novel deformation geometries to determine linear viscoelastic properties. The use of the pseudorandom noise displacements facilitates rapid testing with high data density in the frequency domain. This rapidity is useful, for example, when monitoring changes with time in the rheological properties of a sample (e.g. materials undergoing cure or set). Viscoelastic instruments with a probe-type geometry, such as the imbedded oscillating needle (Sect 3.2), are able to measure properties of materials with solid-like characteristics with minimal sample preparation. The variety of examples presented in this paper (oscillatory squeeze flow (Sect. 3.1), needle (Sect. 3.2), sliding concentric cylinders (Sect.3.3)) demonstrates the wide utility of this general approach.

As discussed in section 2.1, a common feature of the different geometries is that the relation between force ($F^*$) and displacement ($W = W_0 e^{i\omega t}$) has the form $F^* = kG^* W_0$, where $G^*$ is the complex modulus and $k$ is a constant

depending on the instrument geometry. To determine $k$, the correspondence principle of linear viscoelasticity is found to be very useful, since it enables analytical solutions obtained with elastic solids or Newtonian liquids to be converted to the case of a viscoelastic matrix.

The use of pseudorandom noise signals is still comparatively uncommon in rheometry and some of the important issues that should be considered, such as the possibility of aliasing and the use of transfer functions to improve data quality, have been outlined in sections 2.2 and 2.3. As can be seen in the examples presented in section 3, if care is exercised, the general approach described in this paper appears to have great potential for rapid measurement of linear viscoelastic properties of samples which are solid-like or are difficult to prepare into the form required by conventional rotational rheometers. It is hoped that this review stimulates the development of further rheological techniques for efficient characterisation of linear viscoelasticity.

## Acknowledgment

## References

Affrossman, S., D. Hayward, A. McKee, A. Mackinnon, D. Lairez, R.A. Pethrick, A. Vatalis, F.S. Baker and R.E. Carter, 1990, in Carter R.E. (ed.), Rheology of food, Pharmaceutical and biological materials with general rheology, Elsevier, London, 304-314.

Banfill, P.F.G., R.E. Carter and P.J. Weaver, 1991, Simultaneous rheological and kinetic measurements on cement pastes, Cement & Concrete Research 21, 1148-1154.

Bikerman, J.J., 1948, A penetroviscometer for very viscous liquids, J. Colloid Sci. 3, 75-85.

Bird, R.B., R.C. Armstrong and O. Hassager, 1987, Dynamics of polymeric liquids vol.1, 2ed, John Wiley & Sons, New York, p 44.

Bland, D.R., 1960, The theory of linear viscoelasticity, Pergamon, Oxford.

Bracewell, R.N., 2000, The Fourier transform and its applications 3ed, McGraw-Hill, New York.

Christensen, R.M., 1979, Mechanics of composite materials, John Wiley & Sons, New York.

Collyer, A.A. (ed.), 1993, Techniques in rheological measurement, Chapman & Hall, London.

Collyer, A.A. and D.W. Clegg (eds.), 1998, Rheological measurement, 2ed, Chapman & Hall, London.

Cooley, J.W. and J.W. Tukey, 1965, An algorithm for the machine calculation of complex Fourier series, Math. Comp. 19, 297-

301.

Dealy, J.M. and A.J. Giacomin, 1998, Sliding plate and sliding cylinder rheometers, in Collyer A.A. and D.W. Clegg (eds.), rheological measurement, 2ed, Chapman & Hall, London, 237-259.

Ferry, J.D., 1980, Viscoelastic properties of polymers, 3ed, John Wiley & Sons, New York.

Field, J.S., 1995, Determination of materials properties from the deformation of small volumes, PhD Thesis, University of Sydney.

Field, J.S., M.V. Swain and N. Phan-Thien, 1996, An experimental investigation of the use of random squeezing to determine the complex modulus of viscoelastic fluids, J. Non-Newtonian Fluid Mech. 65, 177-194.

Gibson, A.G., G. Kotsikos, J.H. Bland and S. Toll, 1998, Squeeze flow, in Collyer A.A. and D.W. Clegg (eds.), Rheological measurement, 2ed, Chapman Hall, London, 550-592.

Gonsalkorale, S., G. Thomas, H. See and M. Swain, 1999, The viscoelastic properties of alginate hydrocolloid impression material, in Proc. 39th Annual Scientific Meeting of International Association for Dental Research (ANZ Division), Adelaide Australia, 27-29 Sep. 1999, 41.

Haddad, Y.M., 1995, Viscoelasticity of engineering materials, Chapman & Hall, London.

Hashin, Z., 1970, Complex moduli of viscoelastic composites - I. General theory and application to particulate composites, Int. J. Solids Structures 6, 359.

Hibberd, G.E. and N.S. Parker, 1975, Dynamic viscoelastic behavior of wheat flour doughs, Rheol. Acta 14, 151-157.

Hills, D.A., D. Nowell and A. Sackfield, 1993, Mechanics of elastic contacts, Butterworth-Heinemann, Oxford.

Holly, E., S.K. Ventakaram, F. Chambon and H. Winter, 1988, Fourier transform mechanical spectroscopy of viscoelastic materials with transient structure, J. Non-Newtonian Fluid Mech. 27, 17-26.

Honerkamp, J. and J. Weese, 1993, A nonlinear regularization method for the calculation of relaxation spectra, Rheol. Acta 32, 65-73.

Horowitz, P. and W. Hill, 1989, The art of electronics, 2ed., Cambridge University Press, Cambridge.

Hutton, J.F., J.R.A. Pearson and K. Walters (eds.), 1975, Theoretical rheology, Applied Science, London.

Jiang, P., H. See and M. Swain, 2001, Rheological characterisation of dental composite resin cements during curing, to be presented at 3rd Pacific Rim Conference on Rheology, Vancouver Canada, 8-13 July 2001.

Johnson, K.L., 1987, Contact mechanics, Cambridge Univ Press, Cambridge.

Lee, E.H. and J.R.M. Radok, 1960, The contact problem for viscoelastic bodies, Trans. ASME J. Applied Mech. Sept 1960, 438-444.

Goodfriend, M., 1991, Material breakthrough spurs actuator design, Machine Design 63 (March 21 1991), 147-150.

Mackay, M.E., 1993, Rheological measurements on small samples, in Collyer A.A. (ed.), Techniques in Rheological Measurement, Chapman & Hall, London, 225-258.

Mackay, M.E., 1998, Rheological measurements on small sam-

ples, in Collyer A.A. and D.W. Clegg (eds.), Rheological Measurement, 2ed, Chapman & Hall, London, 635-665.

McCarthy, R.V., 1978, An improved rheometer design used to measure viscoelastic properties of polymer melts, J. Rheol. 22, 623-641.

Macosko, C.W., 1994, Rheology principles, measurements, and applications, VCH Publishers, New York.

Nelson, B.I. and J.M. Dealy, 1993, Dynamic mechanical analysis using complex waveforms, in Collyer A.A. (ed.), Techniques in Rheological Measurement, Chapman & Hall, London, 197-224.

Nelson, B.I., T.O. Broadhead, W.I. Paterson and J.M. Dealy, 1994, An in-line melt rheometer for molten plastics, International Polymer Processing 9, 219-224.

Nelson, B.I. and J.M. Dealy, 1998, Dynamic mechanical analysis using complex waveforms, in Collyer A.A. and D.W. Clegg (eds.), Rheological Measurement, 2ed, Chapman & Hall, London, 138-164.

Oka, S., 1960, The principles of rheometry, in Eirich F.R. (ed.), Rheology theory and applications vol. 3, Academic Press, New York, 17-82.

Pethrick, R.A., 1993, Rheological studies using a vibrating probe method, in Collyer A.A. (ed.), Techniques in rheological measurement, Chapman & Hall, London, 161-195.

Pethrick, R.A., 1998, Rheological studies using a vibrating probe, in Collyer A.A. and D.W. Clegg (eds.), Rheological measurement, 2ed, Chapman & Hall, London, 99-137.

Phan-Thien, N. and C.J. Goh, 1981, On the fibre pull-out problem, ZAMM 61, 89-97.

Phan-Thien, N., G. Pantelis and M.B. Bush, 1982, On the elastic fibre pull-out problem, ZAMP 33, 251-265.

Phan-Thien, N. and S. Kim, 1994, Microstructures in elastic media: principles and computational methods, Oxford University Press, New York.

Phan-Thien, N., J.S. Field and M.V. Swain, 1996, Micro-Fourier rheometer: Inertial effects, Rheol. Acta 35, 410-416.

Phan-Thien, N., S. Nasseri and L.E. Bilston, 2000, Oscillatory squeezing flow of a biological material, Rheol. Acta 39, 409-417.

Pipkin, A.C., 1986, Lectures on viscoelasticity theory, Springer Verlag, New York.

Radhakrishnan, S. and R.A. Pethrick, 1994, UV cure monitoring of epoxy-acrylate resins, J. Appl. Polym. Sci. 51, 863-871.

Ramirez, R.W., 1985, The FFT fundamentals and concepts, Prentice-Hall, Englewood Cliffs, New Jersey.

Russel, W.B., 1973, On the effective moduli of composite materials: Effects of fibre length and geometry at dilute concentration, ZAMP 24, 581-600.

Schapery, R.A., 1974, Viscoelastic behavior and analysis of composite materials, in Sendeckyj G.P. (ed.), Composite materials, vol 2, Academic Press, New York.

See, H., J. Field, B. Pfister, M. Swain and N. Phan-Thien, 1997, Electrorheological fluid under squeezing flow, IUTAM 97-9 Rheology and computation, Sydney Australia, 21-25 Jul. 1997.

See, H., C.Y. Ho and N. Phan-Thien, 1998, In situ determination of matrix viscoelasticity of concentrated filler composites, in Nguyen Q.D. and R.R. Huilgol (eds.) 1988, Proc. 8th National

Conf. on Rheol., Adelaide Australia, 19-22 Jul. 195-196.

See, H., J. Field and B. Pfister, 1999a, The response of electrorheological fluid under oscillatory squeeze flow, *J. Non-Newtonian Fluid Mech.* **84**, 149-158.

See, H., A-M. Maher, J.Field, B. Pfister, M. Swain and N. Phan-Thien, 1999b, Measurement of the viscoelastic properties of bituminous materials using an oscillating needle technique, *Rheol. Acta* **38**, 443-450.

See, H., 2000, Using pseudorandom axial oscillations of concentric cylinders to measure the viscoelastic properties of fluids, *Meas. Sci. Technol.* **11**, 1414-1419.

See, H., A-M. Maher, J. Field, B. Pfister, M. Swain and N. Phan-Thien, 2000a, The oscillating needle technique for measuring viscoelastic properties, in Binding D.M., N.E. Hudson, J. Mewis, J.-M. Piau, C.J.S. Petrie, P. Townsend, M.H. Wagner and K. Walters (eds.), Proc. XIIIth International Congress on Rheology, Cambridge UK, 20-25 Aug. 2000, vol. 3, 37-39.

See, H., P. Jiang and N. Phan-Thien, 2000b, Concentration dependence of the linear viscoelastic properties of particle suspensions, *Rheol. Acta* **39**, 131-137.

Shikata, T., H. Niwa and Y. Morishima, 1997, A new system for viscoelastic measurement with mechanical impedance, *J. Soc. Rheol. Japan* **25**, 19-23.

Smith, T.L., J.D. Ferry and F.W. Schremp, 1949, Measurements of the mechanical properties of polymer solutions by electromagnetic transducers, *J. Appl. Phys.* **20**, 144-153.

Swain, M.V., A. Meydan, J.S. Field, B. Pfister, T.J. Bell and R.S. Anderssen, 1997, Development of a microrheometer for binder in pavements, in Proc. 10th Australian Asphalt and Pavement Assoc. International Flexible Pavements Conference, 16-20 Nov 1997, Perth, Australia, 28, 1-13.

Tanner, R.I., 2000, Engineering Rheology, 2ed, Oxford University Press, Oxford.

Tsai, A.T. and D.S. Soong, 1985, Measurement of fast transient and steady-state responses of viscoelastic fluids with a sliding cylinder rheometer executing coaxial displacements, *J. Rheol.* **29**, 1-18.

Van, Loan C., 1992, Computational frameworks for the fast Fourier transform, Society of Industrial and Applied Mathematics, Philadelphia.

Walker, J.S., 1996, Fast Fourier transforms, 2ed, CRC Press, Boca Raton, Florida.

Walters, K., 1974, Rheometry, Chapman and Hall, London.

Whorlow, R.W., 1992, Rheological techniques, 2ed, Ellis Horwood, Chichester.